Dual-Polarized RIS-Based STBC Transmission with Polarization Coupling Analysis

ZHOU Mingyong[1], CHEN Xiangyu[1], TANG Wankai[1], KE Jun Chen[2], JIN Shi[1], CHENG Qiang[2], CUI Tie Jun[2]

(1. National Mobile Communications Research Laboratory, Southeast University, Nanjing 210096, China;
2. State Key Laboratory of Millimeter Waves, Southeast University, Nanjing 210096, China)

DOI: 10.12142/ZTECOM.202201009

https://kns.cnki.net/kcms/detail/34.1294.TN.20220302.1148.002.html, published online March 3, 2022
Manuscript received: 2021-05-12

Abstract: The rapid development of the reconfigurable intelligent surface (RIS) technology has given rise to a new paradigm of wireless transmitters. At present, most research works on RIS-based transmitters focus on single-polarized RISs. In this paper, we propose a dual-polarized RIS-based transmitter, which realizes 4-transmit space-time block coding (STBC) transmission by properly partitioning RIS's unit cells and utilizing the degree of freedom of polarization. The proposed scheme is evaluated through a prototype system that utilizes a fabricated dual-polarized phase-adjustable RIS. In particular, the polarization coupling phenomenon in each unit cell of the employed dual-polarized RIS is modeled and analyzed. The experimental results are in good agreement with the theoretical modeling and analysis results, and an initial research effort is made on characterizing the polarization coupling property in the dual-polarized RIS.

Keywords: reconfigurable intelligent surface; space-time coding; dual polarization; coupling modeling; prototyping

Citation (IEEE Format): M. Y. Zhou, X. Y. Chen, W. K. Tang, et al., "Dual-polarized RIS-based STBC transmission with polarization coupling analysis," *ZTE Communications*, vol. 20, no. 1, pp. 63 - 75, Mar. 2022. doi: 10.12142/ZTECOM.202201009.

1 Introduction

With the commercialization of the fifth-generation (5G) mobile communication networks, the spectrum resources of millimeter wave band are gradually developed and utilized, and base stations (BSs) also begin to assemble massive multiple-input multiple-output (MIMO) hardware and corresponding algorithms to provide better communication services[1-2]. However, the antenna array equipped with massive MIMO needs numerous radio frequency (RF) chains, which leads to high hardware costs, high energy consumption, high system complexity, and severe heat dissipation issues. These problems will become more serious in the sixth-generation (6G) mobile communication networks. The emergence of reconfigurable intelligent surfaces (RISs) in recent years may bring new solutions to these challenges[3-6].

The concept of digital coding and programmable metamaterials was first proposed in 2014[7]. When applied to the field of wireless communications, the reconfigurable two-dimensional metasurfaces are usually called RISs, which are composed of many sub-wavelength unit cells[8-9]. Each unit cell of a RIS can be configured to change its response to electromagnetic (EM) waves, so as to adjust and control EM wave parameters, such as the amplitude or phase, during the interaction between the unit cell and EM waves[10]. A RIS is usually controlled by a field programmable gate array (FPGA) for real-time configuration to realize the regulation and control of EM waves.

The research on RISs can be categorized into two major application directions: the RIS-based transmitter and the RIS-based relay. The RIS-based transmitter focuses on using RIS to regulate EM wave parameters, thus modulating information on EM waves. The RIS-based relay focuses on improving the channel quality through RISs, thus enhancing the signal strength and coverage performance[11-12].

There have been some prior research works on RIS-based transmitters. The authors of Ref. [13] proposed a binary frequency shift keying (BFSK) wireless communication system based on RIS, and the authors of Refs. [14 - 16] realized several RIS-based phase shift keying (PSK) transmission prototypes. A RIS-based space-time transmission system was proposed and implemented in Ref. [17]. However, previous research on RIS-based transmitters was based on single-polarized RISs, and the potential of RISs in the degree of freedom of polarization was not fully exploited. Recently, some fabricated RISs have been able to realize EM control in different polarization directions[18]. The authors of Ref. [19] realized

Corresponding author: JIN Shi
This work was supported by the National Key Research and Development Program of China (2018YFA0701602, 2017YFA0700201, 2017YFA0700202, 2017YFA0700203), the National Natural Science Foundation of China (NSFC) under Grants 61941104, 61921004, 61531011, the Fundamental Research Funds for the Central Universities under Grant 2242022R10062, and the Key Research and Development Program of Shandong Province under Grant 2020CXGC010108.

MIMO transmission based on a dual-polarized RIS, and the authors of Ref. [20] proposed a communication system assisted by a dual-polarized RIS.

In this paper, a 4-transmit space-time block coding (STBC) transmission system based on a dual-polarized RIS is proposed and validated by experiments. In this system, a 4-transmit space-time transmitter is realized by utilizing the degree of freedom of the RIS's polarization. In addition, the polarization coupling phenomenon in the unit cell of the employed dual-polarized RIS is modeled and analyzed.

The rest of the paper is organized as follows. Section 2 introduces the system model of the proposed 4-transmit RIS-based STBC transmission system. Section 3 gives the design details of the proposed system and Section 4 analyzes the bit error rate (BER) performance by considering polarization coupling interference in each unit cell. The prototype system and experimental measurement results are shown in Section 5. Section 6 summarizes the paper.

2 System Model

Fig. 1 shows the diagram of the 4-transmit space-time transmission system based on a dual-polarized RIS. The transmitter consists of a digital baseband module, a dual-polarized phase-adjustable RIS and a radio frequency (RF) signal source. The receiver has K receiving antennas and a baseband processing module. The dual-polarized RIS has N rows and M columns of unit cells, and each unit cell can realize the phase regulation in horizontal polarization and vertical polarization, respectively. M and N are assumed to be even. The single tone carrier signal incident on the dual-polarized RIS is emitted by a feed antenna.

The incident signal power of each unit cell is p in both horizontal and vertical polarization. Let p represent the polarization direction, $p = 1$ means vertical polarization, and $p = 0$ means horizontal polarization. The unit cell in row n and column m is denoted as $U_{n,m}$. $A_{p,n,m}$ and $\varphi_{p,n,m}$ represent the reflection amplitude and reflection phase shift of $U_{n,m}$ in polarization p, and the channel from $U_{n,m}$ to the k-th receiving antenna in polarization p is denoted as $h_k^{p,n,m}$. Then the signal received from $U_{n,m}$ by the k-th receiving antenna in polarization p is $y_k^{p,n,m} = h_k^{p,n,m}\sqrt{P}\,A_{p,n,m}e^{\varphi_{p,n,m}}$. It can be noted that $x_{p,n,m} = A_{p,n,m}e^{\varphi_{p,n,m}}$ represents the data symbol modulated by $U_{n,m}$ onto the single-tone carrier in polarization p and we have $y_k^{p,n,m} = h_k^{p,n,m}\sqrt{P}\,x_{p,n,m}$.

The $n\times m$ unit cells of the RIS can be divided into left and right parts in horizontal polarization, and upper and lower parts in vertical polarization. As shown in Fig. 1, the horizontal left part is marked as the yellow part, the horizontal right part is marked as the orange part, the vertical upper part is marked as the blue part, and the vertical lower part is marked as the indigo part. Then the wireless channel from the yellow part to the k-th receiving antenna is denoted as $h_{k,1} = \sum_{m=1}^{\frac{M}{2}}\sum_{n=1}^{N}h_k^{0,n,m}$, and accordingly, $h_{k,2} = \sum_{m=\frac{M}{2}+1}^{M}\sum_{n=1}^{N}h_k^{0,n,m}$, $h_{k,3} = \sum_{m=1}^{M}\sum_{n=\frac{N}{2}+1}^{N}h_k^{1,n,m}$, and $h_{k,4} = \sum_{m=1}^{M}\sum_{n=1}^{\frac{N}{2}}h_k^{1,n,m}$ stand for the wireless channel between the orange part and the k-th receiving antenna, the wireless channel between the blue part and the k-th receiving antenna, and the wireless channel between the indigo part and the k-th receiving antenna, respectively. Therefore, the

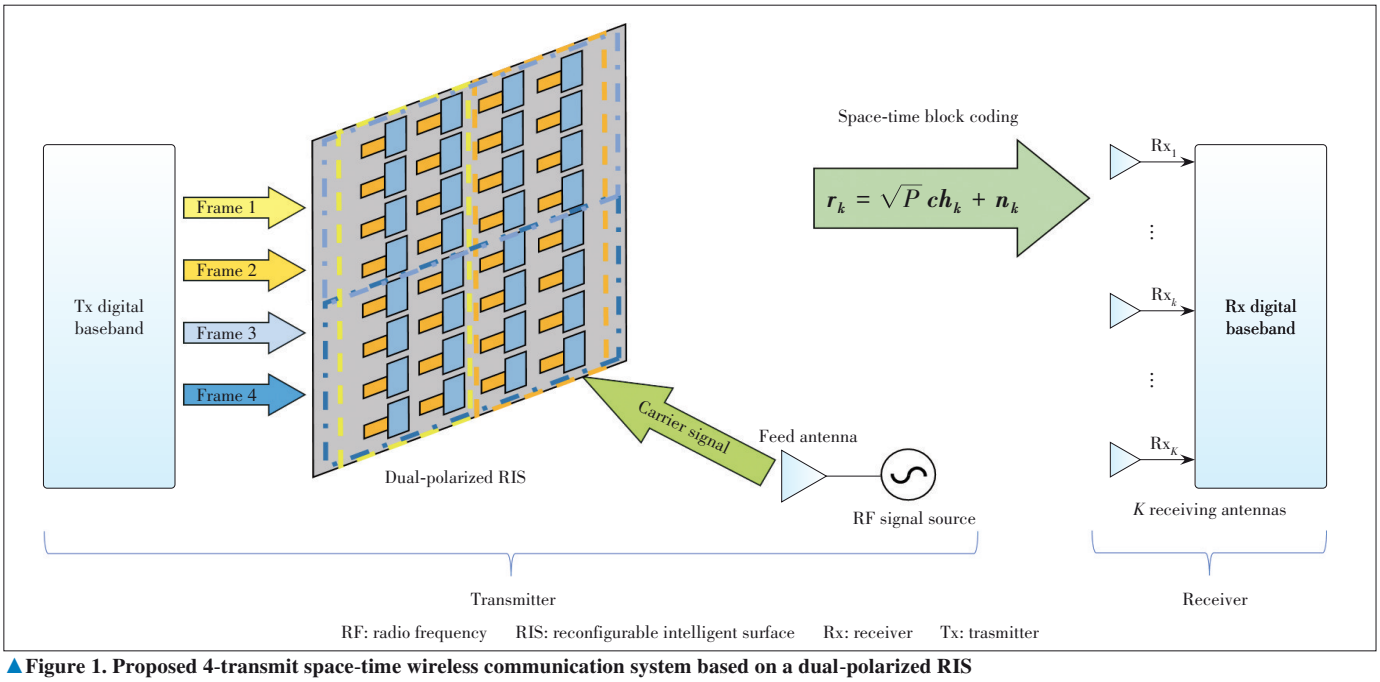

▲**Figure 1. Proposed 4-transmit space-time wireless communication system based on a dual-polarized RIS**

channel parameters from the 4-transmit space-time dual-polarized RIS-based transmitter to the receiver can be written as

$$\boldsymbol{H} = \begin{bmatrix} h_{1,1} & \cdots & h_{K,1} \\ h_{1,2} & \cdots & h_{K,2} \\ h_{1,3} & \cdots & h_{K,3} \\ h_{1,4} & \cdots & h_{K,4} \end{bmatrix}. \tag{1}$$

The STBC matrix is designed as[21]:

$$\boldsymbol{c} = \begin{bmatrix} c_1 & c_2 & c_3 & 0 \\ -c_2^* & c_1^* & 0 & c_3 \\ -c_3^* & 0 & c_1^* & -c_2 \\ 0 & -c_3^* & c_2^* & c_1 \end{bmatrix}, \tag{2}$$

where c_1, c_2, and c_3 are three transmitted baseband symbols. The coding matrix encodes three data streams into four data frames and transmits them in four time slots as a period. The received signals of the k-th receiving antenna in the corresponding time slot of coding are

$$\begin{aligned} r_1^k &= \sqrt{P}\, c_1 h_{k,1} + \sqrt{P}\, c_2 h_{k,2} + \sqrt{P}\, c_3 h_{k,3} + n_1^k, \\ r_2^k &= -\sqrt{P}\, c_2^* h_{k,1} + \sqrt{P}\, c_1^* h_{k,2} + \sqrt{P}\, c_3 h_{k,4} + n_2^k, \\ r_3^k &= -\sqrt{P}\, c_3^* h_{k,1} + \sqrt{P}\, c_1^* h_{k,3} - \sqrt{P}\, c_2 h_{k,4} + n_3^k, \\ r_4^k &= -\sqrt{P}\, c_3^* h_{k,2} + \sqrt{P}\, c_2^* h_{k,3} + \sqrt{P}\, c_1 h_{k,4} + n_4^k, \end{aligned} \tag{3}$$

in which r_i^k is the data received by the k-th receiving antenna in the i-th time slot, and n_i^k is the corresponding receiver noise. In a vector form, let $\boldsymbol{r_k} = \left[r_1^k, r_2^k, r_3^k, r_4^k\right]^{\mathrm{T}}$, $\boldsymbol{n_k} = \left[n_1^k, n_2^k, n_3^k, n_4^k\right]^{\mathrm{T}}$, and $\boldsymbol{h_k} = \left[h_{k,1}, h_{k,2}, h_{k,3}, h_{k,4}\right]^{\mathrm{T}}$, and we have

$$\boldsymbol{r_k} = \sqrt{P}\, \boldsymbol{c}\boldsymbol{h_k} + \boldsymbol{n_k}, \tag{4}$$

where $\boldsymbol{r_k}$, $\boldsymbol{n_k}$ and $\boldsymbol{h_k}$ are the received signal vector, the noise vector, and the wireless channel vector of the k-th antenna, respectively.

Eq. (4) reveals the basic principle of the 4-transmit space-time transmission system based on the dual-polarized RIS. It is consistent with the traditional space-time transmission system in form but different in hardware composition and channel structure. The proposed system modulates the information onto the carrier in the process of reflecting the signal through the dual-polarized RIS, which does not require the conventional RF chains. Therefore, the 4-transmit space-time transmission scheme based on the dual-polarized RIS provides a new space-time transmitter design with the advantages of low hardware costs and complexity.

3 Design of 4-Transmit Space-Time Transmission Based on Dual-Polarized RIS

This section will introduce in detail the scheme of a 4-transmit space-time transmission wireless communication system based on the dual-polarized RIS, including the design of waveforms, the wireless frame structure, and the receiver combining method.

3.1 Waveform Design of Transmitted Symbols

Space-time coding needs to realize the complex conjugate operation of the transmitted symbols. However, the amplitude response and phase shift of the dual-polarized phase-adjustable RIS used in this paper are coupled. If the phase of RIS's unit cell is directly regulated, the envelope of the transmitted symbol will be non-constant and the complex conjugate operation of the symbol cannot be realized. Therefore, the nonlinear modulation technology is employed in this work[17].

During one symbol period, the transmitted symbol waveform is designed as

$$x_{p,n,m}(t) = \begin{cases} e^{j\frac{\Delta\varphi_{p,n,m}}{T_s}\left(T_s - t_{p,n,m} - t\right)}, t \in \left[0, T_s - t_{p,n,m}\right] \\ e^{j\frac{\Delta\varphi_{p,n,m}}{T_s}\left(2T_s - t_{p,n,m} - t\right)}, t \in \left(T_s - t_{p,n,m}, T_s\right] \end{cases}, \tag{5}$$

where T_s is the symbol period, $t_{p,n,m} \in \left[0, T_s\right]$ is the circular time delay, and the symbol phase decreases linearly with $\frac{\Delta\varphi_{p,n,m}}{T_s}$ as the slope.

According to the designed symbol waveform, the amplitude $A_{p,n,m}^{-1}$ and phase $\varphi_{p,n,m}^{-1}$ of the −1-st harmonic with frequency $f_s - \frac{1}{T_s}$ are

$$A_{p,n,m}^{-1} = \left| \mathrm{sinc}\left(\frac{\Delta\varphi_{p,n,m}}{2} - \pi\right) \right|, \tag{6}$$

and

$$\begin{aligned} \varphi_{p,n,m}^{-1} = &-\frac{2\pi t_{p,n,m}}{T_s} + \frac{\Delta\varphi_{p,n,m}}{2} - \pi + \pi \cdot \\ &\mathrm{mod}\left(\left\lfloor \frac{\Delta\varphi_{p,n,m}}{2\pi} - 1 \right\rfloor, 2\right) + \pi \cdot \varepsilon\left(2\pi - \Delta\varphi_{p,n,m}\right), \end{aligned} \tag{7}$$

in which $\mathrm{sinc}(\cdot)$, $\mathrm{mod}(\cdot)$, $\lfloor\cdot\rfloor$, and $\varepsilon(\cdot)$ denote sinc function, modulus operation, round down function and step function, respectively.

3.2 Wireless Frame Structure Design

The frame structure is designed as shown in Fig. 2 for 4-

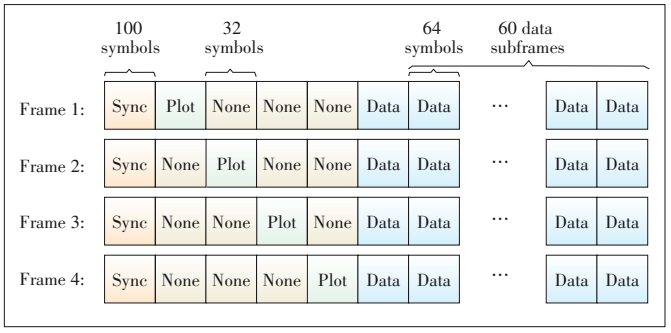

▲ **Figure 2. Frame structure design of 4-transmit space-time transmission system based on dual-polarized RIS**

transmit space-time coding transmission based on the dual-polarized RIS. It includes one synchronization subframe, one pilot subframe and 60 data subframes. The pilots of four transmitting data frames are orthogonal in time for ease of channel estimation. The four data frames are transmitted by the four parts of the RIS respectively. Each pilot subframe includes 32 Binary Phase Shift Keying (BPSK) symbols. There are 64 space-time coded 16-quadrature amplitude modulation (QAM) symbols in each data subframe, and all data symbols are based on the previously described waveform. 11 520 (4×60×64×3/4 = 11 520) data bits are transmitted per frame duration.

3.3 Combining Scheme of Receiver

When the receiver has only one receiving antenna (K=1), we have

$$\begin{aligned}
r_1^1 &= \sqrt{P}\,c_1 h_{1,1} + \sqrt{P}\,c_2 h_{1,2} + \sqrt{P}\,c_3 h_{1,3} + n_1^1,\\
r_2^1 &= -\sqrt{P}\,c_2^* h_{1,1} + \sqrt{P}\,c_1^* h_{1,2} + \sqrt{P}\,c_3 h_{1,4} + n_2^1,\\
r_3^1 &= -\sqrt{P}\,c_3^* h_{1,1} + \sqrt{P}\,c_1^* h_{1,3} - \sqrt{P}\,c_2 h_{1,4} + n_3^1,\\
r_4^1 &= -\sqrt{P}\,c_3^* h_{1,2} + \sqrt{P}\,c_2^* h_{1,3} + \sqrt{P}\,c_1 h_{1,4} + n_4^1,
\end{aligned} \tag{8}$$

where c_1, c_2, and c_3 are the source symbols satisfying $\mathbb{E}\left\{\left|c_1\right|^2\right\} = \mathbb{E}\left\{\left|c_2\right|^2\right\} = \mathbb{E}\left\{\left|c_3\right|^2\right\} = 1$, and $\mathbb{E}\{\cdot\}$ represents expectation operation. n_1^1, n_2^1, n_3^1, and n_4^1 denote independent complex Gaussian noises with zero mean and variance σ^2.

By applying the combination scheme in Ref. [22], we have

$$\tilde{c}_1 = \frac{r_1^1 h_{1,1}^* + r_2^{1*} h_{1,2} + r_3^{1*} h_{1,3} + r_4^1 h_{1,4}^*}{\left(\left|h_{1,1}\right|^2 + \left|h_{1,2}\right|^2 + \left|h_{1,3}\right|^2 + \left|h_{1,4}\right|^2\right)\sqrt{P}} = c_1 + \frac{n_1^1 h_{1,1}^* + n_2^{1*} h_{1,2} + n_3^{1*} h_{1,3} + n_4^1 h_{1,4}^*}{\left(\left|h_{1,1}\right|^2 + \left|h_{1,2}\right|^2 + \left|h_{1,3}\right|^2 + \left|h_{1,4}\right|^2\right)\sqrt{P}}, \tag{9}$$

$$\tilde{c}_2 = \frac{r_1^1 h_{1,2}^* - r_2^{1*} h_{1,1} - r_3^1 h_{1,4}^* + r_4^{1*} h_{1,3}}{\left(\left|h_{1,1}\right|^2 + \left|h_{1,2}\right|^2 + \left|h_{1,3}\right|^2 + \left|h_{1,4}\right|^2\right)\sqrt{P}} = c_2 + \frac{n_1^1 h_{1,2}^* - n_2^{1*} h_{1,1} - n_3^1 h_{1,4}^* + n_4^{1*} h_{1,3}}{\left(\left|h_{1,1}\right|^2 + \left|h_{1,2}\right|^2 + \left|h_{1,3}\right|^2 + \left|h_{1,4}\right|^2\right)\sqrt{P}},$$

$$\tilde{c}_3 = \frac{r_1^1 h_{1,3}^* + r_2^1 h_{1,4}^* - r_3^{1*} h_{1,1} - r_4^{1*} h_{1,2}}{\left(\left|h_{1,1}\right|^2 + \left|h_{1,2}\right|^2 + \left|h_{1,3}\right|^2 + \left|h_{1,4}\right|^2\right)\sqrt{P}} = c_3 + \frac{n_1^1 h_{1,3}^* + n_2^1 h_{1,4}^* - n_3^{1*} h_{1,1} - n_4^{1*} h_{1,2}}{\left(\left|h_{1,1}\right|^2 + \left|h_{1,2}\right|^2 + \left|h_{1,3}\right|^2 + \left|h_{1,4}\right|^2\right)\sqrt{P}},$$

where $\tilde{c}_1, \tilde{c}_2$ and $\tilde{c}_3$ represent the recovered symbols of three data streams. According to the above formulas, when the receiver has only one receiving antenna, the signal-to-noise ratio (SNR) of stream 1, stream 2 and stream 3 is

$$\mathrm{SNR}_1^{1\mathrm{Rx}} = \mathrm{SNR}_2^{1\mathrm{Rx}} = \mathrm{SNR}_3^{1\mathrm{Rx}} = \frac{\left(\left|h_{1,1}\right|^2 + \left|h_{1,2}\right|^2 + \left|h_{1,3}\right|^2 + \left|h_{1,4}\right|^2\right)P}{\sigma^2}. \tag{10}$$

Similarly, when there are two receiving antennas, according to the combining scheme in Ref. [22], there are

$$\tilde{c}_1 = \frac{r_1^1 h_{1,1}^* + r_2^{1*} h_{1,2} + r_3^{1*} h_{1,3} + r_4^1 h_{1,4}^* + r_1^2 h_{2,1}^* + r_2^{2*} h_{2,2} + r_3^{2*} h_{2,3} + r_4^2 h_{2,4}^*}{\left(\left|h_{1,1}\right|^2 + \left|h_{1,2}\right|^2 + \left|h_{1,3}\right|^2 + \left|h_{1,4}\right|^2 + \left|h_{2,1}\right|^2 + \left|h_{2,2}\right|^2 + \left|h_{2,3}\right|^2 + \left|h_{2,4}\right|^2\right)\sqrt{P}} = c_1 + \frac{n_1^1 h_{1,1}^* + n_2^{1*} h_{1,2} + n_3^{1*} h_{1,3} + n_4^1 h_{1,4}^* + n_1^2 h_{2,1}^* + n_2^{2*} h_{2,2} + n_3^{2*} h_{2,3} + n_4^2 h_{2,4}^*}{\left(\left|h_{1,1}\right|^2 + \left|h_{1,2}\right|^2 + \left|h_{1,3}\right|^2 + \left|h_{1,4}\right|^2 + \left|h_{2,1}\right|^2 + \left|h_{2,2}\right|^2 + \left|h_{2,3}\right|^2 + \left|h_{2,4}\right|^2\right)\sqrt{P}}, \tag{11}$$

$$\tilde{c}_2 = \frac{r_1^1 h_{1,2}^* - r_2^{1*} h_{1,1} - r_3^1 h_{1,4}^* + r_4^{1*} h_{1,3} + r_1^2 h_{2,2}^* - r_2^{2*} h_{2,1} - r_3^2 h_{2,4}^* + r_4^{2*} h_{2,3}}{\left(\left|h_{1,1}\right|^2 + \left|h_{1,2}\right|^2 + \left|h_{1,3}\right|^2 + \left|h_{1,4}\right|^2 + \left|h_{2,1}\right|^2 + \left|h_{2,2}\right|^2 + \left|h_{2,3}\right|^2 + \left|h_{2,4}\right|^2\right)\sqrt{P}} = c_2 + \frac{n_1^1 h_{1,2}^* - n_2^{1*} h_{1,1} - n_3^1 h_{1,4}^* + n_4^{1*} h_{1,3} + n_1^2 h_{2,2}^* - n_2^{2*} h_{2,1} - n_3^2 h_{2,4}^* + n_4^{2*} h_{2,3}}{\left(\left|h_{1,1}\right|^2 + \left|h_{1,2}\right|^2 + \left|h_{1,3}\right|^2 + \left|h_{1,4}\right|^2 + \left|h_{2,1}\right|^2 + \left|h_{2,2}\right|^2 + \left|h_{2,3}\right|^2 + \left|h_{2,4}\right|^2\right)\sqrt{P}}, \tag{12}$$

$$\tilde{c}_3 = \frac{r_1^1 h_{1,3}^* + r_2^1 h_{1,4}^* - r_3^{1*} h_{1,1} - r_4^{1*} h_{1,2} + r_1^2 h_{2,3}^* + r_2^{2*} h_{2,4}^* - r_3^{2*} h_{2,1} - r_4^{2*} h_{2,2}}{\left(\left|h_{1,1}\right|^2 + \left|h_{1,2}\right|^2 + \left|h_{1,3}\right|^2 + \left|h_{1,4}\right|^2 + \left|h_{2,1}\right|^2 + \left|h_{2,2}\right|^2 + \left|h_{2,3}\right|^2 + \left|h_{2,4}\right|^2\right)\sqrt{P}} = c_3 + \frac{n_1^1 h_{1,3}^* + n_2^1 h_{1,4}^* - n_3^{1*} h_{1,1} - n_4^{1*} h_{1,2} + n_1^2 h_{2,3}^* + n_2^{2*} h_{2,4}^* - n_3^{2*} h_{2,1} - n_4^{2*} h_{2,2}}{\left(\left|h_{1,1}\right|^2 + \left|h_{1,2}\right|^2 + \left|h_{1,3}\right|^2 + \left|h_{1,4}\right|^2 + \left|h_{2,1}\right|^2 + \left|h_{2,2}\right|^2 + \left|h_{2,3}\right|^2 + \left|h_{2,4}\right|^2\right)\sqrt{P}}. \tag{13}$$

Therefore, when there are two receiving antennas at the receiver, the SNR of stream 1, stream 2 and stream 3 is

$$\mathrm{SNR}_1^{2\mathrm{Rx}} = \mathrm{SNR}_2^{2\mathrm{Rx}} = \mathrm{SNR}_3^{2\mathrm{Rx}} = \frac{\left(\left|h_{1,1}\right|^2 + \left|h_{1,2}\right|^2 + \left|h_{1,3}\right|^2 + \left|h_{1,4}\right|^2 + \left|h_{2,1}\right|^2 + \left|h_{2,2}\right|^2 + \left|h_{2,3}\right|^2 + \left|h_{2,4}\right|^2\right)P}{\sigma^2}. \quad (14)$$

From the two SNR formulas of Eqs. (10) and (14), it can be found that the 4-transmit space-time transmission scheme based on the dual-polarized RIS proposed in this paper is basically consistent with the traditional space-time transmission system. The same diversity order and diversity gain can be obtained.

4 Polarization Coupling Modeling and BER Performance Analysis

4.1 Polarization Coupling Modeling for Dual-Polarized RIS

The authors of Ref. [19] have preliminarily revealed the phenomenon of polarization coupling in the unit cell of the dual-polarized RIS. Based on the coupling constellation and the coupling voltage of the unit cell given in Ref. [19], a linear symbolic coupling model is proposed as follows to analyze the polarization coupling phenomenon in the 4-transmit space-time transmission based on the dual-polarized RIS.

Theorem 1. The coupling model between two polarization directions of the unit cell $U_{n,m}$ can be written as

$$\begin{cases} x_{couple}^{0,n,m} = x_{0,n,m} + a x_{1,n,m} \\ x_{couple}^{1,n,m} = x_{1,n,m} + b x_{0,n,m} \end{cases}, \quad (15)$$

where a and b are the coefficients coupled to the horizontal and vertical polarization, $x_{0,n,m}$and $x_{1,n,m}$ are the original transmitted symbols in horizontal and vertical polarization, and $x_{couple}^{0,n,m}$ and $x_{couple}^{1,n,m}$ are the actual transmitted symbols in horizontal and vertical polarization.

Theorem 1 reveals that the transmitted symbols of two polarization directions are mutually coupled in one unit cell of the dual-polarized RIS. In particular, Theorem 1 indicates that the actual transmitted symbols are the linear combination of original transmitted symbols and coupled transmitted symbols from another polarization direction.

Based on the system model in Section 2, when the system operates normally and has no polarization coupling interference, the signal received from $U_{n,m}$ by the k-th receiving antenna in polarization p is $y_k^{p,n,m} = h_k^{p,n,m}\sqrt{P}\,x_{p,n,m}$.

According to Theorem 1, the signal that considers polarization coupling interference received from $U_{n,m}$ by the k-th receiving antenna in polarization p is $y_{couple}^{k,p,n,m} = h_k^{p,n,m}\sqrt{P}\,x_{p,n,m} + q h_k^{p,n,m}\sqrt{P}\,x_{1-p,n,m}$, where $x_{1-p,n,m}$ is the transmitted symbol in another polarization, and q is the coupling coefficient between unit cell's control voltages for horizontal and vertical polarization directions. According to Ref. [19], $q = a = \frac{1.01}{6}$ is the coefficient coupled to the horizontal polarization and $q = b = \frac{0.92}{8}$ is the coefficient coupled to the vertical polarization for the employed dual-polarized RIS.

4.2 BER Performance Without Polarization Coupling Interference

For the sake of analysis, it is assumed that the wireless channel parameters $\left(h_{1,1}, h_{1,2}, h_{1,3}, h_{1,4}, h_{2,1}, h_{2,2}, h_{2,3}, h_{2,4}\right)$ remain constant during transmission. Due to the standardly mapped 16-QAM with Gray coding and the traditional QAM demodulation method, the theoretical total BER of the 4-transmit space-time RIS-based transmission system can be expressed as[17, 23]:

$$\mathrm{BER}_{1\mathrm{Rx}} \cong \frac{3}{8}\mathrm{erfc}\left(\sqrt{\frac{4\mathrm{SNR}_{\mathrm{Rx1}}}{30}}\right) + \frac{1}{4}\mathrm{erfc}\left(3\sqrt{\frac{4\mathrm{SNR}_{\mathrm{Rx1}}}{30}}\right), \quad (16)$$

$$\mathrm{SNR}_{\mathrm{Rx1}} = \frac{3\left(\left|h_{1,1}\right|^2 + \left|h_{1,2}\right|^2 + \left|h_{1,3}\right|^2 + \left|h_{1,4}\right|^2\right)P}{4\sigma^2}, \quad (17)$$

where $\mathrm{erfc}(\cdot)$ is the complementary error function and $\mathrm{SNR}_{\mathrm{Rx1}}$ is the received SNR for one receiving antenna.

Similarly, the system BER with two receiving antennas is[17, 23]:

$$\mathrm{BER}_{2\mathrm{Rx}} \cong \frac{3}{8}\mathrm{erfc}\left(\sqrt{\frac{4\beta\,\mathrm{SNR}_{\mathrm{Rx1}}}{30}}\right) + \frac{1}{4}\mathrm{erfc}\left(3\sqrt{\frac{4\beta\,\mathrm{SNR}_{\mathrm{Rx1}}}{30}}\right), \quad (18)$$

$$\beta = \frac{\left|h_{1,1}\right|^2 + \left|h_{1,2}\right|^2 + \left|h_{1,3}\right|^2 + \left|h_{1,4}\right|^2 + \left|h_{2,1}\right|^2 + \left|h_{2,2}\right|^2 + \left|h_{2,3}\right|^2 + \left|h_{2,4}\right|^2}{\left|h_{1,1}\right|^2 + \left|h_{1,2}\right|^2 + \left|h_{1,3}\right|^2 + \left|h_{1,4}\right|^2}, \quad (19)$$

where β is the diversity gain obtained when the receiver has two receiving antennas.

4.3 BER Performance Considering Polarization Coupling Interference

Take the horizontal polarization as an example, when the symbols X_1, X_2, X_3 and X_4 are respectively transmitted by the yellow, orange, blue and indigo parts of RIS as shown in Fig. 1 in a certain time slot, the signal received by the k-th receiving antenna in horizontal polarization from the yellow part is

$$y_{yellow}^{k,0} = \sum_{m=1}^{\frac{M}{2}}\sum_{n=1}^{N} h_k^{0,n,m}\sqrt{P}\,X_1 +$$
$$a\sum_{m=1}^{\frac{M}{2}}\sum_{n=\frac{N}{2}+1}^{N} h_k^{0,n,m}\sqrt{P}\,X_3 + a\sum_{m=1}^{\frac{M}{2}}\sum_{n=1}^{\frac{N}{2}} h_k^{0,n,m}\sqrt{P}\,X_4 =$$
$$h_{k,1}\sqrt{P}\,X_1 + a\sum_{m=1}^{\frac{M}{2}}\sum_{n=\frac{N}{2}+1}^{N} h_k^{0,n,m}\sqrt{P}\,X_3 + a\sum_{m=1}^{\frac{M}{2}}\sum_{n=1}^{\frac{N}{2}} h_k^{0,n,m}\sqrt{P}\,X_4 =$$
$$h_{k,1}\sqrt{P}\,X_1 + ah_k^{upper,yellow}\sqrt{P}\,X_3 + ah_k^{lower,yellow}\sqrt{P}\,X_4, \quad (20)$$

where $h_k^{upper,yellow} = \sum_{m=1}^{\frac{M}{2}}\sum_{n=\frac{N}{2}+1}^{N} h_k^{0,n,m}$ and $h_k^{lower,yellow} = \sum_{m=1}^{\frac{M}{2}}\sum_{n=1}^{\frac{N}{2}} h_k^{0,n,m}$ are the channels from the upper region and lower region of the yellow part to the k-th receiving antenna in horizontal polarization.

And the signal received by the k-th receiving antenna in horizontal polarization from the orange part is

$$y_{orange}^{k,0} = \sum_{m=\frac{M}{2}+1}^{M}\sum_{n=1}^{N} h_k^{0,n,m}\sqrt{P}\,X_2 +$$
$$a\sum_{m=\frac{M}{2}+1}^{M}\sum_{n=\frac{N}{2}+1}^{N} h_k^{0,n,m}\sqrt{P}\,X_3 + a\sum_{m=\frac{M}{2}+1}^{M}\sum_{n=1}^{\frac{N}{2}} h_k^{0,n,m}\sqrt{P}\,X_4 =$$
$$h_{k,2}\sqrt{P}\,X_2 + a\sum_{m=\frac{M}{2}+1}^{M}\sum_{n=\frac{N}{2}+1}^{N} h_k^{0,n,m}\sqrt{P}\,X_3 +$$
$$a\sum_{m=\frac{M}{2}+1}^{M}\sum_{n=1}^{\frac{N}{2}} h_k^{0,n,m}\sqrt{P}\,X_4 =$$
$$h_{k,2}\sqrt{P}\,X_2 + ah_k^{upper,orange}\sqrt{P}\,X_3 + ah_k^{lower,orange}\sqrt{P}\,X_4, \quad (21)$$

where $h_k^{upper,orange} = \sum_{m=\frac{M}{2}+1}^{M}\sum_{n=\frac{N}{2}+1}^{N} h_k^{0,n,m}$ and $h_k^{lower,orange} = \sum_{m=\frac{M}{2}+1}^{M}\sum_{n=1}^{\frac{N}{2}} h_k^{0,n,m}$ are the channels from the upper region and lower region of the orange part to the k-th receiving antenna in horizontal polarization.

Due to the proposed wireless frame structure and transmission scheme, $h_k^{upper,yellow}$, $h_k^{lower,yellow}$, $h_k^{upper,orange}$ and $h_k^{lower,orange}$ cannot be estimated and obtained. Because receiving antennas are placed approximately on the central normal line of the RIS, we can assume that $h_k^{upper,yellow} \approx \frac{1}{2}h_{k,1}$, $h_k^{lower,yellow} \approx \frac{1}{2}h_{k,1}$, $h_k^{upper,orange} \approx \frac{1}{2}h_{k,2}$, and $h_k^{lower,orange} \approx \frac{1}{2}h_{k,2}$, and Eqs. (18) and (19) can be written as

$$y_{yellow}^{k,0} = h_{k,1}\sqrt{P}\,X_1 + a\sum_{m=1}^{\frac{M}{2}}\sum_{n=\frac{N}{2}+1}^{N} h_k^{0,n,m}\sqrt{P}\,X_3 +$$
$$a\sum_{m=1}^{\frac{M}{2}}\sum_{n=1}^{\frac{N}{2}} h_k^{0,n,m}\sqrt{P}\,X_4 \approx h_{k,1}\sqrt{P}\,X_1 +$$
$$a\left(\frac{1}{2}h_{k,1}\right)\sqrt{P}\,X_3 + a\left(\frac{1}{2}h_{k,1}\right)\sqrt{P}\,X_4 =$$
$$h_{k,1}\sqrt{P}\left(X_1 + \frac{1}{2}aX_3 + \frac{1}{2}aX_4\right), \quad (22)$$

and

$$y_{orange}^{k,0} \approx h_{k,2}\sqrt{P}\left(X_2 + \frac{1}{2}aX_3 + \frac{1}{2}aX_4\right). \quad (23)$$

Similarly, for the blue and indigo parts, we have

$$y_{blue}^{k,1} \approx h_{k,3}\sqrt{P}\left(X_3 + \frac{1}{2}bX_1 + \frac{1}{2}bX_2\right), \quad (24)$$

and

$$y_{indigo}^{k,1} \approx h_{k,4}\sqrt{P}\left(X_4 + \frac{1}{2}bX_1 + \frac{1}{2}bX_2\right). \quad (25)$$

For the k-th receiving antenna, the received signal in a certain time slot is

$$y_k = y_{yellow}^{k,0} + y_{orange}^{k,0} + y_{blue}^{k,1} + y_{indigo}^{k,1}$$
$$\approx \sqrt{P}\left[\begin{array}{l} h_{k,1}\left(X_1 + \frac{1}{2}aX_3 + \frac{1}{2}aX_4\right) + \\ h_{k,2}\left(X_2 + \frac{1}{2}aX_3 + \frac{1}{2}aX_4\right) + \\ h_{k,3}\left(X_3 + \frac{1}{2}bX_1 + \frac{1}{2}bX_2\right) + h_{k,4}\left(X_4 + \frac{1}{2}bX_1 + \frac{1}{2}bX_2\right)\end{array}\right] =$$
$$\sqrt{P}\,\boldsymbol{h_k}\boldsymbol{X}\boldsymbol{Q}_{couple} = \sqrt{P}\,\boldsymbol{h_k}\boldsymbol{X}_{couple}, \quad (26)$$

where $\boldsymbol{h_k} = \left[h_{k,1}, h_{k,2}, h_{k,3}, h_{k,4}\right]^{\mathrm{T}}$, $\boldsymbol{X} = \left[X_1, X_2, X_3, X_4\right]$, and

$$\boldsymbol{Q}_{couple} = \begin{bmatrix} 1 & 0 & \frac{1}{2}b & \frac{1}{2}b \\ 0 & 1 & \frac{1}{2}b & \frac{1}{2}b \\ \frac{1}{2}a & \frac{1}{2}a & 1 & 0 \\ \frac{1}{2}a & \frac{1}{2}a & 0 & 1 \end{bmatrix}, \quad (27)$$

$$\boldsymbol{X}_{couple} = \boldsymbol{X}\boldsymbol{Q}_{couple} = \left[X_1 + \frac{1}{2}aX_3 + \frac{1}{2}aX_4, X_2 + \frac{1}{2}aX_3 + \frac{1}{2}aX_4, X_3 + \frac{1}{2}bX_1 + \frac{1}{2}bX_2, X_4 + \frac{1}{2}bX_1 + \frac{1}{2}bX_2\right].$$

When the RIS-based transmitter transmits data according to the STBC matrix $\boldsymbol{c}$ of Eq. (2), we let $u = \frac{1}{2}a$, $v = \frac{1}{2}b$ and there is

$$\boldsymbol{c}_{couple} = \boldsymbol{c}\boldsymbol{Q}_{couple} = \begin{bmatrix} c_1 + uc_3 & c_2 + uc_3 & c_3 + vc_1 + vc_2 & vc_1 + vc_2 \\ -c_2^* + uc_3 & c_1^* + uc_3 & -vc_2^* + vc_1^* & c_3 - vc_2^* + vc_1^* \\ -c_3^* + uc_1^* - uc_2 & uc_1^* - uc_2 & c_1^* - vc_3^* & -c_2 - vc_3^* \\ uc_2^* + uc_1 & -c_3^* + uc_2^* + uc_1 & c_2^* - vc_3^* & c_1 - vc_3^* \end{bmatrix}. \quad (28)$$

Then we have

$$\boldsymbol{r}_{couple}^{\boldsymbol{k}} = \sqrt{P}\,\boldsymbol{c}_{couple}\boldsymbol{h}_{\boldsymbol{k}} + \boldsymbol{n}_{\boldsymbol{k}}, \quad (29)$$

where $\boldsymbol{r}_{couple}^{\boldsymbol{k}} = \left[r_{couple}^{k,1}, r_{couple}^{k,2}, r_{couple}^{k,3}, r_{couple}^{k,4}\right]^T$ is the received signal vector considering polarization coupling interference.

Eq. (27) gives the system model that considers polarization coupling interference, and the influence of the proposed symbolic coupling model is mainly reflected in the STBC matrix $\boldsymbol{c}_{couple}$. Then the BER performance of the system is discussed as follows.

Proposition 1. When considering polarization coupling interference and there is only one receiving antenna at the receiver, the upper bound of system BER can be written as

$$\mathrm{BER}_{upbound}^{1\mathrm{Rx}} \cong \frac{3}{8}\mathrm{erfc}\left(\sqrt{\frac{\mathrm{SINR}^{1\mathrm{Rx}}}{10}}\right) + \frac{1}{4}\mathrm{erfc}\left(3\sqrt{\frac{\mathrm{SINR}^{1\mathrm{Rx}}}{10}}\right), \quad (30)$$

$$\mathrm{SINR}^{1\mathrm{Rx}} = \frac{1}{\frac{3}{4\,\mathrm{SNR}_{\mathrm{Rx1}}} + \frac{4\left(u^2\left|h_{1,1}\right|^2 + u^2\left|h_{1,2}\right|^2 + v^2\left|h_{1,3}\right|^2 + v^2\left|h_{1,4}\right|^2\right)}{3\left(\left|h_{1,1}\right|^2 + \left|h_{1,2}\right|^2 + \left|h_{1,3}\right|^2 + \left|h_{1,4}\right|^2\right)} + \frac{\left(u^2 + v^2\right)\left(\left|h_{1,1}\right|^2 + \left|h_{1,2}\right|^2\right)\left(\left|h_{1,3}\right|^2 + \left|h_{1,4}\right|^2\right)}{3\left(\left|h_{1,1}\right|^2 + \left|h_{1,2}\right|^2 + \left|h_{1,3}\right|^2 + \left|h_{1,4}\right|^2\right)^2}}, \quad (31)$$

where $\mathrm{SINR}^{1\mathrm{Rx}}$ is the signal-to-interference plus noise ratio (SINR) of the data stream with a single receiving antenna.

Proof: See Appendix A.

Eq. (28) in Proposition 1 and Eq. (16) have the same structure, but the difference is that Eq. (28) is related to SINR due to the polarization coupling interference while Eq. (16) is just related to SNR. Proposition 1 reveals that the BER of the proposed system is not only influenced by the SNR of the system, but also by polarization coupling interference. When the interference terms in SINR are 0, Eq. (28) will degenerate into Eq. (16). However, because of the interference terms, the SINR of the system will decrease, which leads to the deterioration of the system BER performance and this is consistent with the intuition.

For the case of two receiving antennas, we can get Proposition 2 as follows.

Proposition 2: When considering polarization coupling interference and there are two receiving antennas at the receiver, the upper bound of system BER can be written as

$$\mathrm{BER}_{upbound}^{2\mathrm{Rx}} \cong \frac{3}{8}\mathrm{erfc}\left(\sqrt{\frac{\mathrm{SINR}^{2\mathrm{Rx}}}{10}}\right) + \frac{1}{4}\mathrm{erfc}\left(3\sqrt{\frac{\mathrm{SINR}^{2\mathrm{Rx}}}{10}}\right), \quad (32)$$

$$\mathrm{SINR}^{2\mathrm{Rx}} = \frac{1}{\frac{3}{4\beta\,\mathrm{SNR}_{\mathrm{Rx1}}} + d_1 + d_2 + d_3}, \quad (33)$$

where $\mathrm{SINR}^{2\mathrm{Rx}}$ is the SINR of system data stream with two receiving antennas and

$$d_1 = \frac{4\left[\left(u^2\left|h_{1,1}\right|^2 + u^2\left|h_{1,2}\right|^2 + v^2\left|h_{1,3}\right|^2 + v^2\left|h_{1,4}\right|^2\right)\left(\left|h_{1,1}\right|^2 + \left|h_{1,2}\right|^2 + \left|h_{1,3}\right|^2 + \left|h_{1,4}\right|^2\right)\right]}{3\left(\left|h_{1,1}\right|^2 + \left|h_{1,2}\right|^2 + \left|h_{1,3}\right|^2 + \left|h_{1,4}\right|^2 + \left|h_{2,1}\right|^2 + \left|h_{2,2}\right|^2 + \left|h_{2,3}\right|^2 + \left|h_{2,4}\right|^2\right)^2},$$

$$d_2 = \frac{4\left[\left(u^2\left|h_{2,1}\right|^2 + u^2\left|h_{2,2}\right|^2 + v^2\left|h_{2,3}\right|^2 + v^2\left|h_{2,4}\right|^2\right)\left(\left|h_{2,1}\right|^2 + \left|h_{2,2}\right|^2 + \left|h_{2,3}\right|^2 + \left|h_{2,4}\right|^2\right)\right]}{3\left(\left|h_{1,1}\right|^2 + \left|h_{1,2}\right|^2 + \left|h_{1,3}\right|^2 + \left|h_{1,4}\right|^2 + \left|h_{2,1}\right|^2 + \left|h_{2,2}\right|^2 + \left|h_{2,3}\right|^2 + \left|h_{2,4}\right|^2\right)^2},$$

$$d_3 = \frac{\left(u^2 + v^2\right)\left[\left(\left|h_{1,1}\right|^2 + \left|h_{1,2}\right|^2\right)\left(\left|h_{1,3}\right|^2 + \left|h_{1,4}\right|^2\right) + \left(\left|h_{2,1}\right|^2 + \left|h_{2,2}\right|^2\right)\left(\left|h_{2,3}\right|^2 + \left|h_{2,4}\right|^2\right)\right]}{3\left(\left|h_{1,1}\right|^2 + \left|h_{1,2}\right|^2 + \left|h_{1,3}\right|^2 + \left|h_{1,4}\right|^2 + \left|h_{2,1}\right|^2 + \left|h_{2,2}\right|^2 + \left|h_{2,3}\right|^2 + \left|h_{2,4}\right|^2\right)^2}.$$

Proof: See Appendix B.

According to Proposition 2, diversity gain β exists in both SNR terms and interference terms (d_1, d_2, d_3), which means that even if more receiving antennas are equipped, polarization coupling interference will still prominently affect the BER performance of the system. Besides, Eqs. (28) and (29) also indicate that if we want to improve the BER performance, we need to reduce coupling coefficients u and v, which leads to less polarization coupling interference. And that puts forward new requirements for the design of the unit cell of a dual-polarized RIS. In the following section, we will validate the proposed symbolic polarization coupling model by the experi-

mental measurements based on our prototype system.

5 Implementation of 4-Transmit Space-Time Transmission Based on Dual-Polarized RIS

5.1 Prototype Setup

Fig. 3 shows our prototype of 4-transmit space-time transmission based on the dual-polarized RIS. The system consists of a 4-transmit space-time RIS-based transmitter and a traditional receiver. The 4-transmit space-time transmitter is composed of a dual-polarized phase-adjustable RIS that is controled by a PXIe platform, a horn antenna and an RF signal source. The traditional receiver consists of two receiving antennas and a software defined radio (SDR) platform.

The dual-polarized RIS is a phase programmable metasurface with an operating frequency of 2.7 GHz. There are 144 (12×12) unit cells in total, and each unit cell has two pairs of metal patches and two varactor diodes are connected across it. The bias voltage is applied to the varactor diodes through the corresponding metal patches to control the reflection coefficient of the unit cell in two polarization directions[18 - 19]. The RIS fabricated with varactors can continuously regulate the phase, which makes the transmission waveform design in Section 4 achievable.

Specifically, three bit streams are generated by the PXIe platform, mapped into three 16-QAM symbol streams, and encoded by the STBC matrix to generate four baseband frames. The four frames are converted into four analog voltage signals by the digital-to-analog converters (DACs) of the PXIe platform and loaded on the varactors of the corresponding RIS's unit cells respectively. When the 2.7 GHz single tone carrier generated by the RF signal source is transmitted and irradiated on the RIS through the horn antenna, the dual-polarized RIS modulates four data frames onto the carrier. The transmitting horn antenna is placed at an inclination of 45° so that there are carrier components in both horizontal and vertical polarization directions. The receiver receives the signal through two single polarization antennas inclined at 45°. The received signal is down converted and sampled on the SDR platform, and the corresponding baseband data symbols are then decoded and demodulated.

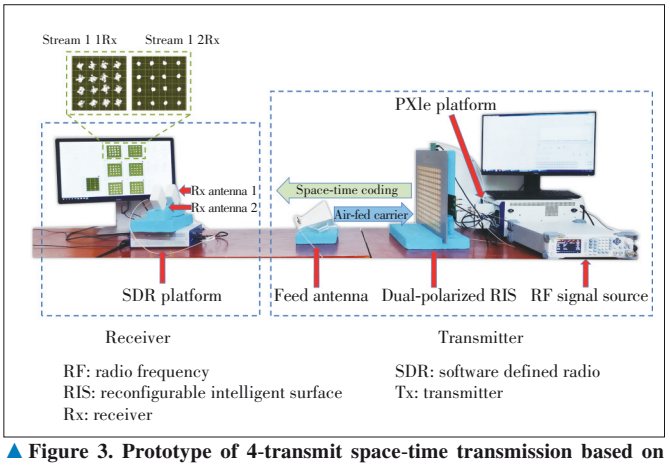

▲ **Figure 3. Prototype of 4-transmit space-time transmission based on dual-polarized RIS**

5.2 Experimental Results

As shown in Fig. 3, the 4-transmit space-time transmission system based on the dual-polarized RIS can successfully realize data transmission. The prototype is in an indoor environment with a transmission distance of about 1.5 m. When the symbol rate of the system is 2.5 million symbol/s, the transmission rate can reach 7.5 Mbit/s, which is determined by the adopted space-time coding scheme. It can be seen from Fig. 3 that the constellations of three data streams at the receiver can be well recovered. By adjusting the transmission power to change the received SNR, the BER performance is recorded simultaneously. The measurement results are shown in Fig. 4. In Fig. 4, the blue line is the theoretical BER curve without polarization coupling interference, the red line is the upper bound of the theoretical BER considering polarization coupling interference, and the orange line is the actual measured BER curve. It can be seen that the measured BER is obviously worse than the theoretical one without polarization coupling interference. This is because the control voltages regulating the unit cell's phase in different polarization directions are coupled[19], which makes the four data frames doped with each other in the transmission process, resulting in additional interference and degradation of the BER performance of the actual system. Fig. 4 also shows that the theoretical BER upper bounds given in Eqs. (28) and (29) are in good agreement with the measured curve, which validates our proposed linear symbol polarization coupling model for the dual-polarized RIS.

The above results indicate that the 4-transmit space-time transmission scheme based on the dual-polarized phase-adjustable RIS is feasible, but the mutual coupling of control voltages of the unit cell for different polarization directions will degrade the system performance. This enlightens that the polarization isolation performance should be carefully considered when designing dual-polarized RISs, and it is worth further exploring in the future.

6 Conclusions

In this paper, a 4-transmit space-time transmission scheme based on the dual-polarized RIS is proposed. The prototype system based on a dual-polarized phase-adjustable RIS can transmit data over the air at a rate of 7.5 Mbit/s, which verifies the feasibility of the proposed scheme. In particular, a simple linear symbolic polarization coupling model is proposed for theoretical analysis, and the BER performance upper bound of the system is given. The measured curves are in good agreement with the theoretical ones, which proves the effectiveness of the proposed model and scheme. In general, a multi-transmit space-time transmitter based on the dual-polarized

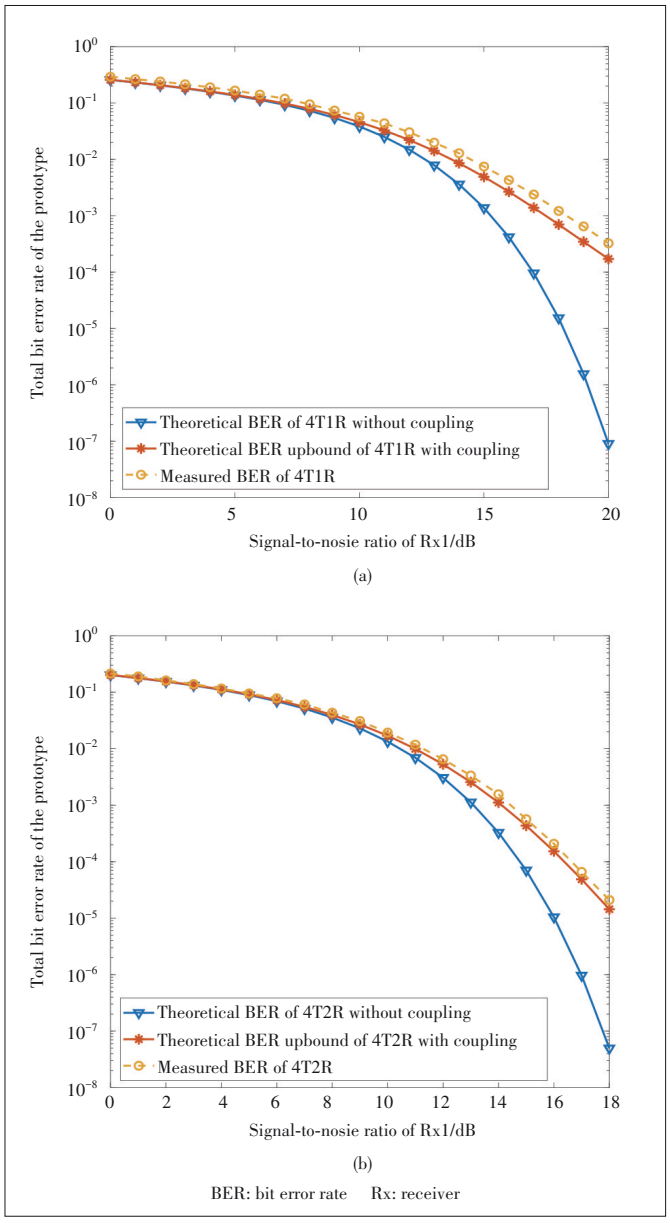

▲**Figure 4. Comparison of system theoretical and measured BER-SNR performance: (a) one receiving antenna and (b) two receiving antennas**

RIS is a promising scheme, which can flexibly build different space-time transmission systems to satisfy the transmission requirements with low hardware complexity and cost.

Appendix A

Proof of Proposition 1

The STBC matrix considering polarization coupling interference is shown in Eq. (26). When K=1, which means that the receiver has only one receiving antenna, it can be obtained from Eq. (27) that

$$r_{couple}^{1,1} = \sqrt{P}\,h_{1,1}\left(c_1 + uc_3\right) + \sqrt{P}\,h_{1,2}\left(c_2 + uc_3\right) + \sqrt{P}\,h_{1,3}\left(c_3 + vc_1 + vc_2\right) + \sqrt{P}\,h_{1,4}\left(vc_1 + vc_2\right) + n_1^1,$$

$$r_{couple}^{1,2} = \sqrt{P}\,h_{1,1}\left(-c_2^* + uc_3\right) + \sqrt{P}\,h_{1,2}\left(c_1^* + uc_3\right) + \sqrt{P}\,h_{1,3}\left(-vc_2^* + vc_1^*\right) + \sqrt{P}\,h_{1,4}\left(c_3 - vc_2^* + vc_1^*\right) + n_2^1,$$

$$r_{couple}^{1,3} = \sqrt{P}\,h_{1,1}\left(-c_3^* + uc_1^* - uc_2\right) + \sqrt{P}\,h_{1,2}\left(uc_1^* - uc_2\right) + \sqrt{P}\,h_{1,3}\left(c_1^* - vc_3^*\right) + \sqrt{P}\,h_{1,4}\left(-c_2 - vc_3^*\right) + n_3^1,$$

$$r_{couple}^{1,4} = \sqrt{P}\,h_{1,1}\left(uc_2^* + uc_1\right) + \sqrt{P}\,h_{1,2}\left(-c_3^* + uc_2^* + uc_1\right) + \sqrt{P}\,h_{1,3}\left(c_2^* - vc_3^*\right) + \sqrt{P}\,h_{1,4}\left(c_1 - vc_3^*\right) + n_4^1.$$

According to Ref. [22], there are the following combination formulas.

$$\tilde{c}_{1,couple} = r_{couple}^{1,1}h_{1,1}^* + r_{couple}^{1,2*}h_{1,2} + r_{couple}^{1,3*}h_{1,3} + r_{couple}^{1,4}h_{1,4}^*,$$

$$\tilde{c}_{2,couple} = r_{couple}^{1,1}h_{1,2}^* - r_{couple}^{1,2*}h_{1,1} - r_{couple}^{1,3}h_{1,4}^* + r_{couple}^{1,4*}h_{1,3},$$

$$\tilde{c}_{3,couple} = r_{couple}^{1,1}h_{1,3}^* + r_{couple}^{1,2}h_{1,4}^* - r_{couple}^{1,3*}h_{1,1} - r_{couple}^{1,4*}h_{1,2}.$$

By substituting $r_{couple}^{1,1}$, $r_{couple}^{1,2}$, $r_{couple}^{1,3}$, and $r_{couple}^{1,4}$ into the combination formula of $\tilde{c}_{1,couple}$, we have:

$$\begin{aligned}\tilde{c}_{1,couple} &= r_{couple}^{1,1}h_{1,1}^* + r_{couple}^{1,2*}h_{1,2} + r_{couple}^{1,3*}h_{1,3} + r_{couple}^{1,4}h_{1,4}^* = \\ &\sqrt{P}\left[\left(c_1 + uc_3\right)\left|h_{1,1}\right|^2 + \left(c_2 + uc_3\right)h_{1,2}h_{1,1}^* + \left(c_3 + vc_1 + vc_2\right)h_{1,3}h_{1,1}^* + \left(vc_1 + vc_2\right)h_{1,4}h_{1,1}^*\right] + n_1^1h_{1,1}^* = \\ &\sqrt{P}\left[\left(-c_2^* + uc_3\right)^*h_{1,1}^*h_{1,2} + \left(c_1^* + uc_3\right)^*\left|h_{1,2}\right|^2 + \left(-vc_2^* + vc_1^*\right)^*h_{1,3}^*h_{1,2} + \left(c_3 - vc_2^* + vc_1^*\right)^*h_{1,4}^*h_{1,2}\right] + n_2^{1*}h_{1,2} + \\ &\sqrt{P}\left[\left(-c_3^* + uc_1^* - uc_2\right)^*h_{1,1}^*h_{1,3} + \left(uc_1^* - uc_2\right)^*h_{1,2}^*h_{1,3} + \left(c_1^* - vc_3^*\right)^*\left|h_{1,3}\right|^2 + \left(-c_2 - vc_3^*\right)^*h_{1,4}^*h_{1,3}\right] + n_3^{1*}h_{1,3} + \\ &\sqrt{P}\left[\left(uc_2^* + uc_1\right)h_{1,1}h_{1,4}^* + \left(-c_3^* + uc_2^* + uc_1\right)h_{1,2}h_{1,4}^* + \left(c_2^* - vc_3^*\right)h_{1,3}h_{1,4}^* + \left(c_1 - vc_3^*\right)\left|h_{1,4}\right|^2\right] + n_4^1h_{1,4}^*\end{aligned}.$$

Sort out the expression of $\tilde{c}_{1,couple}$ and we have

$$\tilde{c}_{1,couple} = c_1\sqrt{P}\left(\left|h_{1,1}\right|^2+\left|h_{1,2}\right|^2+\left|h_{1,3}\right|^2+\left|h_{1,4}\right|^2\right)+$$
$$c_1\sqrt{P}\left[u\left(h_{1,2}h_{1,4}^*+h_{1,1}^*h_{1,3}+h_{1,1}h_{1,4}^*+h_{1,2}^*h_{1,3}\right)+\right.$$
$$\left.v\left(h_{1,2}h_{1,4}^*+h_{1,1}^*h_{1,3}+h_{1,3}^*h_{1,2}+h_{1,4}h_{1,1}^*\right)\right]+$$
$$c_2\sqrt{P}\,v\left(h_{1,1}^*h_{1,3}+h_{1,4}h_{1,1}^*-h_{1,3}^*h_{1,2}-h_{1,2}h_{1,4}^*\right)+$$
$$c_2^*\sqrt{P}\,u\left(h_{1,1}h_{1,4}^*+h_{1,2}h_{1,4}^*-h_{1,1}^*h_{1,3}-h_{1,2}^*h_{1,3}\right)+$$
$$c_3\sqrt{P}\left[u\left(\left|h_{1,1}\right|^2+h_{1,1}^*h_{1,2}\right)-v\left(\left|h_{1,3}\right|^2+h_{1,3}h_{1,4}^*\right)\right]+$$
$$c_3^*\sqrt{P}\left[u\left(\left|h_{1,2}\right|^2+h_{1,1}^*h_{1,2}\right)-v\left(\left|h_{1,4}\right|^2+h_{1,3}h_{1,4}^*\right)\right]+$$
$$n_1^1h_{1,1}^*+n_2^{1*}h_{1,2}+n_3^{1*}h_{1,3}+n_4^1h_{1,4}^*\ .$$

Let $\tilde{c}_{signal}^{1,couple} = c_1\sqrt{P}\left(\left|h_{1,1}\right|^2+\left|h_{1,2}\right|^2+\left|h_{1,3}\right|^2+\left|h_{1,4}\right|^2\right)$, $\tilde{c}_{noise}^{1,couple} = n_1^1h_{1,1}^*+n_2^{1*}h_{1,2}+n_3^{1*}h_{1,3}+n_4^1h_{1,4}^*$,

$$\tilde{c}_{interference}^{1,couple} = c_1\sqrt{P}\left[u\left(h_{1,2}h_{1,4}^*+h_{1,1}^*h_{1,3}+h_{1,1}h_{1,4}^*+h_{1,2}^*h_{1,3}\right)+\right.$$
$$\left.v\left(h_{1,2}h_{1,4}^*+h_{1,1}^*h_{1,3}+h_{1,3}^*h_{1,2}+h_{1,4}h_{1,1}^*\right)\right]+$$
$$c_2\sqrt{P}\,v\left(h_{1,1}^*h_{1,3}+h_{1,4}h_{1,1}^*-h_{1,3}^*h_{1,2}-h_{1,2}h_{1,4}^*\right)+$$
$$c_2^*\sqrt{P}\,u\left(h_{1,1}h_{1,4}^*+h_{1,2}h_{1,4}^*-h_{1,1}^*h_{1,3}-h_{1,2}^*h_{1,3}\right)+$$
$$c_3\sqrt{P}\left[u\left(\left|h_{1,1}\right|^2+h_{1,1}^*h_{1,2}\right)-v\left(\left|h_{1,3}\right|^2+h_{1,3}h_{1,4}^*\right)\right]+$$
$$c_3^*\sqrt{P}\left[u\left(\left|h_{1,2}\right|^2+h_{1,1}^*h_{1,2}\right)-v\left(\left|h_{1,4}\right|^2+h_{1,3}h_{1,4}^*\right)\right].$$

From the inequality property $\left(x_1+x_2\right)^2 \geqslant x_1^2+x_2^2$, we can get

$$\left|u\left(h_{1,2}h_{1,4}^*+h_{1,1}^*h_{1,3}+h_{1,1}h_{1,4}^*+h_{1,2}^*h_{1,3}\right)+\right.$$
$$\left.v\left(h_{1,2}h_{1,4}^*+h_{1,1}^*h_{1,3}+h_{1,3}^*h_{1,2}+h_{1,4}h_{1,1}^*\right)\right|^2 \geqslant$$
$$\left(u^2+v^2\right)\left(\left|h_{1,2}\right|^2\left|h_{1,4}\right|^2+\left|h_{1,1}\right|^2\left|h_{1,3}\right|^2+\right.$$
$$\left.\left|h_{1,1}\right|^2\left|h_{1,4}\right|^2+\left|h_{1,2}\right|^2\left|h_{1,3}\right|^2\right),$$

$$\left|h_{1,1}^*h_{1,3}+h_{1,4}h_{1,1}^*-h_{1,3}^*h_{1,2}-h_{1,2}h_{1,4}^*\right|^2 \geqslant \left|h_{1,2}\right|^2\left|h_{1,4}\right|^2+$$
$$\left|h_{1,1}\right|^2\left|h_{1,3}\right|^2+\left|h_{1,1}\right|^2\left|h_{1,4}\right|^2+\left|h_{1,2}\right|^2\left|h_{1,3}\right|^2,$$

$$\left|h_{1,1}h_{1,4}^*+h_{1,2}h_{1,4}^*-h_{1,1}^*h_{1,3}-h_{1,2}^*h_{1,3}\right|^2 \geqslant \left|h_{1,2}\right|^2\left|h_{1,4}\right|^2+$$
$$\left|h_{1,1}\right|^2\left|h_{1,3}\right|^2+\left|h_{1,1}\right|^2\left|h_{1,4}\right|^2+\left|h_{1,2}\right|^2\left|h_{1,3}\right|^2,$$

$$\left|u\left(\left|h_{1,1}\right|^2+h_{1,1}^*h_{1,2}\right)-v\left(\left|h_{1,3}\right|^2+h_{1,3}h_{1,4}^*\right)\right|^2 \geqslant u^2\left(\left|h_{1,1}\right|^4+\right.$$
$$\left.\left|h_{1,1}\right|^2\left|h_{1,2}\right|^2\right)+v^2\left(\left|h_{1,3}\right|^4+\left|h_{1,3}\right|^2\left|h_{1,4}\right|^2\right),$$

$$\left|u\left(\left|h_{1,2}\right|^2+h_{1,1}^*h_{1,2}\right)-v\left(\left|h_{1,4}\right|^2+h_{1,3}h_{1,4}^*\right)\right|^2 \geqslant u^2\left(\left|h_{1,2}\right|^4+\right.$$
$$\left.\left|h_{1,1}\right|^2\left|h_{1,2}\right|^2\right)+v^2\left(\left|h_{1,4}\right|^4+\left|h_{1,3}\right|^2\left|h_{1,4}\right|^2\right).$$

Then we have

$$P_{interference}^{\tilde{c}_{1,couple}} = E\left[\left(\tilde{c}_{interference}^{1,couple}\right)^2\right] \geqslant$$
$$P\left[2\left(u^2+v^2\right)\left(\begin{array}{c}\left|h_{1,2}\right|^2\left|h_{1,4}\right|^2+\left|h_{1,1}\right|^2\left|h_{1,3}\right|^2+\left|h_{1,1}\right|^2\left|h_{1,4}\right|^2\\+\left|h_{1,2}\right|^2\left|h_{1,3}\right|^2\end{array}\right)+\right.$$
$$u^2\left(\left|h_{1,1}\right|^4+\left|h_{1,1}\right|^2\left|h_{1,2}\right|^2\right)+v^2\left(\left|h_{1,3}\right|^4+\left|h_{1,3}\right|^2\left|h_{1,4}\right|^2\right)+$$
$$\left.u^2\left(\left|h_{1,2}\right|^4+\left|h_{1,1}\right|^2\left|h_{1,2}\right|^2\right)+v^2\left(\left|h_{1,4}\right|^4+\left|h_{1,3}\right|^2\left|h_{1,4}\right|^2\right)\right] =$$
$$P\left[u^2\left|h_{1,1}\right|^4+u^2\left|h_{1,2}\right|^4+v^2\left|h_{1,3}\right|^4+v^2\left|h_{1,4}\right|^4+\right.$$
$$2u^2\left(\left|h_{1,1}\right|^2\left|h_{1,2}\right|^2+\left|h_{1,1}\right|^2\left|h_{1,3}\right|^2+\left|h_{1,1}\right|^2\left|h_{1,4}\right|^2+\right.$$
$$\left.\left|h_{1,2}\right|^2\left|h_{1,3}\right|^2+\left|h_{1,2}\right|^2\left|h_{1,4}\right|^2\right)+$$
$$\left.2v^2\left(\begin{array}{c}\left|h_{1,1}\right|^2\left|h_{1,2}\right|^2+\left|h_{1,1}\right|^2\left|h_{1,3}\right|^2+\left|h_{1,1}\right|^2\left|h_{1,4}\right|^2+\\\left|h_{1,2}\right|^2\left|h_{1,3}\right|^2+\left|h_{1,2}\right|^2\left|h_{1,4}\right|^2\end{array}\right)\right] =$$
$$P\left(u^2+v^2\right)\left(\left|h_{1,1}\right|^2+\left|h_{1,2}\right|^2\right)\left(\left|h_{1,3}\right|^2+\left|h_{1,4}\right|^2\right)+$$
$$P\left(u^2\left|h_{1,1}\right|^2+u^2\left|h_{1,2}\right|^2+v^2\left|h_{1,3}\right|^2+\right.$$
$$\left.v^2\left|h_{1,4}\right|^2\right)\left(\left|h_{1,1}\right|^2+\left|h_{1,2}\right|^2+\left|h_{1,3}\right|^2+\left|h_{1,4}\right|^2\right),$$

$$P_{signal}^{\tilde{c}_{1,couple}} = E\left[\left(\tilde{c}_{signal}^{1,couple}\right)^2\right] = P\left(\left|h_{1,1}\right|^2+\left|h_{1,2}\right|^2+\left|h_{1,3}\right|^2+\left|h_{1,4}\right|^2\right)^2,$$

$$P_{noise}^{\tilde{c}_{1,couple}} = E\left[\left(\tilde{c}_{noise}^{1,couple}\right)^2\right] = \sigma^2\left(\left|h_{1,1}\right|^2+\left|h_{1,2}\right|^2+\left|h_{1,3}\right|^2+\left|h_{1,4}\right|^2\right).$$

Similarly, for

$$\tilde{c}_{2,couple} = r_{couple}^{1,1}h_{1,2}^*-r_{couple}^{1,2*}h_{1,1}-r_{couple}^{1,3}h_{1,4}^*+r_{couple}^{1,4*}h_{1,3},$$
$$\tilde{c}_{3,couple} = r_{couple}^{1,1}h_{1,3}^*+r_{couple}^{1,2}h_{1,4}^*-r_{couple}^{1,3*}h_{1,1}-r_{couple}^{1,4*}h_{1,2},$$

there are

$$P_{interference}^{\tilde{c}_{2,couple}} = E\left[\left(\tilde{c}_{interference}^{2,couple}\right)^2\right] \geqslant P\left(u^2+v^2\right)\left(\left|h_{1,1}\right|^2+\left|h_{1,2}\right|^2\right)\left(\left|h_{1,3}\right|^2+\left|h_{1,4}\right|^2\right)+P\left(u^2\left|h_{1,1}\right|^2+u^2\left|h_{1,2}\right|^2+v^2\left|h_{1,3}\right|^2+v^2\left|h_{1,4}\right|^2\right)\left(\left|h_{1,1}\right|^2+\left|h_{1,2}\right|^2+\left|h_{1,3}\right|^2+\left|h_{1,4}\right|^2\right).$$

$$P_{signal}^{\tilde{c}_{2,couple}} = E\left[\left(\tilde{c}_{signal}^{2,couple}\right)^2\right] = P\left(\left|h_{1,1}\right|^2+\left|h_{1,2}\right|^2+\left|h_{1,3}\right|^2+\left|h_{1,4}\right|^2\right)^2,$$

$$P_{noise}^{\tilde{c}_{2,couple}} = E\left[\left(\tilde{c}_{noise}^{2,couple}\right)^2\right] = \sigma^2\left(\left|h_{1,1}\right|^2+\left|h_{1,2}\right|^2+\left|h_{1,3}\right|^2+\left|h_{1,4}\right|^2\right),$$

$$P_{interference}^{\tilde{c}_{3,couple}} = E\left[\left(\tilde{c}_{interference}^{3,couple}\right)^2\right] \geqslant P\left[u^2\left(\left|h_{1,1}\right|^2+\left|h_{1,2}\right|^2\right)^2+v^2\left(\left|h_{1,3}\right|^2+\left|h_{1,4}\right|^2\right)^2\right]+P\left(u^2\left|h_{1,1}\right|^2+u^2\left|h_{1,2}\right|^2+v^2\left|h_{1,3}\right|^2+v^2\left|h_{1,4}\right|^2\right)\left(\left|h_{1,1}\right|^2+\left|h_{1,2}\right|^2+\left|h_{1,3}\right|^2+\left|h_{1,4}\right|^2\right),$$

$$P_{signal}^{\tilde{c}_{3,couple}} = E\left[\left(\tilde{c}_{signal}^{3,couple}\right)^2\right] = P\left(\left|h_{1,1}\right|^2+\left|h_{1,2}\right|^2+\left|h_{1,3}\right|^2+\left|h_{1,4}\right|^2\right)^2,$$

$$P_{noise}^{\tilde{c}_{3,couple}} = E\left[\left(\tilde{c}_{noise}^{3,couple}\right)^2\right] = \sigma^2\left(\left|h_{1,1}\right|^2+\left|h_{1,2}\right|^2+\left|h_{1,3}\right|^2+\left|h_{1,4}\right|^2\right).$$

Then,

$$\mathrm{SINR}^{1\mathrm{Rx}} = \frac{P_{signal}^{\tilde{c}_{1,couple}}+P_{signal}^{\tilde{c}_{2,couple}}+P_{signal}^{\tilde{c}_{3,couple}}}{P_{noise}^{\tilde{c}_{1,couple}}+P_{noise}^{\tilde{c}_{2,couple}}+P_{noise}^{\tilde{c}_{3,couple}}+P_{interference}^{\tilde{c}_{1,couple}}+P_{interference}^{\tilde{c}_{2,couple}}+P_{interference}^{\tilde{c}_{3,couple}}} \leqslant \frac{1}{\frac{3}{4\,\mathrm{SNR}_{\mathrm{Rx1}}}+\frac{4\left(u^2\left|h_{1,1}\right|^2+u^2\left|h_{1,2}\right|^2+v^2\left|h_{1,3}\right|^2+v^2\left|h_{1,4}\right|^2\right)}{3\left(\left|h_{1,1}\right|^2+\left|h_{1,2}\right|^2+\left|h_{1,3}\right|^2+\left|h_{1,4}\right|^2\right)}+\frac{\left(u^2+v^2\right)\left(\left|h_{1,1}\right|^2+\left|h_{1,2}\right|^2\right)\left(\left|h_{1,3}\right|^2+\left|h_{1,4}\right|^2\right)}{3\left(\left|h_{1,1}\right|^2+\left|h_{1,2}\right|^2+\left|h_{1,3}\right|^2+\left|h_{1,4}\right|^2\right)^2}}.$$

Appendix B

Proof of Proposition 2

When K=2, the received signals on the second receiving antenna can be obtained from Eq. (27):

$$r_{couple}^{2,1} = \sqrt{P}\,h_2\left(c_1+uc_3\right)+\sqrt{P}\,h_{2,2}\left(c_2+uc_3\right)+\sqrt{P}\,h_{2,3}\left(c_3+vc_1+vc_2\right)+\sqrt{P}\,h_{2,4}\left(vc_1+vc_2\right)+n_1^2,$$

$$r_{couple}^{2,2} = \sqrt{P}\,h_{2,1}\left(-c_2^*+uc_3\right)+\sqrt{P}\,h_{2,2}\left(c_1^*+uc_3\right)+\sqrt{P}\,h_{2,3}\left(-vc_2^*+vc_1^*\right)+\sqrt{P}\,h_{2,4}\left(c_3-vc_2^*+vc_1^*\right)+n_2^2,$$

$$r_{couple}^{2,3} = \sqrt{P}\,h_{2,1}\left(-c_3^*+uc_1^*-uc_2\right)+\sqrt{P}\,h_{2,2}\left(uc_1^*-uc_2\right)+\sqrt{P}\,h_{2,3}\left(c_1^*-vc_3^*\right)+\sqrt{P}\,h_{2,4}\left(-c_2-vc_3^*\right)+n_3^2,$$

$$r_{couple}^{2,4} = \sqrt{P}\,h_{2,1}\left(uc_2^*+uc_1\right)+\sqrt{P}\,h_{2,2}\left(-c_3^*+uc_2^*+uc_1\right)+\sqrt{P}\,h_{2,3}\left(c_2^*-vc_3^*\right)+\sqrt{P}\,h_{2,4}\left(c_1-vc_3^*\right)+n_4^2.$$

According to Ref. [22], for two receiving antennas, there are the following combination formulas:

$$\tilde{c}_{1,couple} = r_1^1h_{1,1}^*+r_2^{1*}h_{1,2}+r_3^{1*}h_{1,3}+r_4^1h_{1,4}^*+r_1^2h_{2,1}^*+r_2^{2*}h_{2,2}+r_3^{2*}h_{2,3}+r_4^2h_{2,4}^*,$$

$$\tilde{c}_{2,couple} = r_1^1h_{1,2}^*-r_2^{1*}h_{1,1}-r_3^1h_{1,4}^*+r_4^{1*}h_{1,3}+r_1^2h_{2,2}^*-r_2^{2*}h_{2,1}-r_3^2h_{2,4}^*+r_4^{2*}h_{2,3},$$

$$\tilde{c}_{3,couple} = r_1^1h_{1,3}^*+r_2^1h_{1,4}^*-r_3^{1*}h_{1,1}-r_4^{1*}h_{1,2}+r_1^2h_{2,3}^*+r_2^2h_{2,4}^*-r_3^{2*}h_{2,1}-r_4^{2*}h_{2,2}.$$

Since the form and structure of the received signals of the two antennas are consistent, the signal processing of the two receiving antennas is consistent in the combination formula. Therefore, it is easy to obtain

$$P_{interference}^{\tilde{c}_{1,couple}} = P_{interference}^{\tilde{c}_{2,couple}} \geqslant P\left(u^2+v^2\right)\left(\left|h_{1,1}\right|^2+\left|h_{1,2}\right|^2\right)\left(\left|h_{1,3}\right|^2+\left|h_{1,4}\right|^2\right)+P\left(u^2\left|h_{1,1}\right|^2+u^2\left|h_{1,2}\right|^2+v^2\left|h_{1,3}\right|^2+v^2\left|h_{1,4}\right|^2\right)\left(\left|h_{1,1}\right|^2+\left|h_{1,2}\right|^2+\left|h_{1,3}\right|^2+\left|h_{1,4}\right|^2\right)+P\left(u^2+v^2\right)\left(\left|h_{2,1}\right|^2+\left|h_{2,2}\right|^2\right)\left(\left|h_{2,3}\right|^2+\left|h_{2,4}\right|^2\right)+P\left(u^2\left|h_{2,1}\right|^2+u^2\left|h_{2,2}\right|^2+v^2\left|h_{2,3}\right|^2+v^2\left|h_{2,4}\right|^2\right)\left(\left|h_{2,1}\right|^2+\left|h_{2,2}\right|^2+\left|h_{2,3}\right|^2+\left|h_{2,4}\right|^2\right),$$

$$P_{interference}^{\tilde{c}_{3,couple}} \geqslant P\left[u^2\left(\left|h_{1,1}\right|^2+\left|h_{1,2}\right|^2\right)^2+v^2\left(\left|h_{1,3}\right|^2+\left|h_{1,4}\right|^2\right)^2\right]+P\left(u^2\left|h_{1,1}\right|^2+u^2\left|h_{1,2}\right|^2+v^2\left|h_{1,3}\right|^2+v^2\left|h_{1,4}\right|^2\right)\left(\left|h_{1,1}\right|^2+\left|h_{1,2}\right|^2+\left|h_{1,3}\right|^2+\left|h_{1,4}\right|^2\right)+P\left[u^2\left(\left|h_{2,1}\right|^2+\left|h_{2,2}\right|^2\right)^2+v^2\left(\left|h_{2,3}\right|^2+\left|h_{2,4}\right|^2\right)^2\right]+P\left(u^2\left|h_{2,1}\right|^2+u^2\left|h_{2,2}\right|^2+v^2\left|h_{2,3}\right|^2+v^2\left|h_{2,4}\right|^2\right)\left(\left|h_{2,1}\right|^2+\left|h_{2,2}\right|^2+\left|h_{2,3}\right|^2+\left|h_{2,4}\right|^2\right),$$

$$P_{signal}^{\tilde{c}_{1,couple}}=P_{signal}^{\tilde{c}_{2,couple}}=P_{signal}^{\tilde{c}_{3,couple}}=P\left(\left|h_{1,1}\right|^2+\left|h_{1,2}\right|^2+\left|h_{1,3}\right|^2+\left|h_{1,4}\right|^2+\left|h_{2,1}\right|^2+\left|h_{2,2}\right|^2+\left|h_{2,3}\right|^2+\left|h_{2,4}\right|^2\right)^2,$$

$$P_{noise}^{\tilde{c}_{1,couple}}=P_{noise}^{\tilde{c}_{2,couple}}=P_{noise}^{\tilde{c}_{3,couple}}=\sigma^2\left(\left|h_{1,1}\right|^2+\left|h_{1,2}\right|^2+\left|h_{1,3}\right|^2+\left|h_{1,4}\right|^2+\left|h_{2,1}\right|^2+\left|h_{2,2}\right|^2+\left|h_{2,3}\right|^2+\left|h_{2,4}\right|^2\right).$$

Then we have

$$\mathrm{SINR}^{2\mathrm{Rx}}=\frac{P_{signal}^{\tilde{c}_{1,couple}}+P_{signal}^{\tilde{c}_{2,couple}}+P_{signal}^{\tilde{c}_{3,couple}}}{P_{noise}^{\tilde{c}_{1,couple}}+P_{noise}^{\tilde{c}_{2,couple}}+P_{noise}^{\tilde{c}_{3,couple}}+P_{interference}^{\tilde{c}_{1,couple}}+P_{interference}^{\tilde{c}_{2,couple}}+P_{interference}^{\tilde{c}_{3,couple}}}\leqslant\frac{1}{\frac{3}{4\beta\,\mathrm{SNR}_{\mathrm{Rx1}}}+d_1+d_2+d_3},$$

where $\beta=\frac{\left|h_{1,1}\right|^2+\left|h_{1,2}\right|^2+\left|h_{1,3}\right|^2+\left|h_{1,4}\right|^2+\left|h_{2,1}\right|^2+\left|h_{2,2}\right|^2+\left|h_{2,3}\right|^2+\left|h_{2,4}\right|^2}{\left|h_{1,1}\right|^2+\left|h_{1,2}\right|^2+\left|h_{1,3}\right|^2+\left|h_{1,4}\right|^2}$ is the diversity gain and

$$d_1=\frac{4\left[\left(u^2\left|h_{1,1}\right|^2+u^2\left|h_{1,2}\right|^2+v^2\left|h_{1,3}\right|^2+v^2\left|h_{1,4}\right|^2\right)\left(\left|h_{1,1}\right|^2+\left|h_{1,2}\right|^2+\left|h_{1,3}\right|^2+\left|h_{1,4}\right|^2\right)\right]}{3\left(\left|h_{1,1}\right|^2+\left|h_{1,2}\right|^2+\left|h_{1,3}\right|^2+\left|h_{1,4}\right|^2+\left|h_{2,1}\right|^2+\left|h_{2,2}\right|^2+\left|h_{2,3}\right|^2+\left|h_{2,4}\right|^2\right)^2},$$

$$d_2=\frac{4\left[\left(u^2\left|h_{2,1}\right|^2+u^2\left|h_{2,2}\right|^2+v^2\left|h_{2,3}\right|^2+v^2\left|h_{2,4}\right|^2\right)\left(\left|h_{2,1}\right|^2+\left|h_{2,2}\right|^2+\left|h_{2,3}\right|^2+\left|h_{2,4}\right|^2\right)\right]}{3\left(\left|h_{1,1}\right|^2+\left|h_{1,2}\right|^2+\left|h_{1,3}\right|^2+\left|h_{1,4}\right|^2+\left|h_{2,1}\right|^2+\left|h_{2,2}\right|^2+\left|h_{2,3}\right|^2+\left|h_{2,4}\right|^2\right)^2},$$

$$d_3=\frac{\left(u^2+v^2\right)\left[\left(\left|h_{1,1}\right|^2+\left|h_{1,2}\right|^2\right)\left(\left|h_{1,3}\right|^2+\left|h_{1,4}\right|^2\right)+\left(\left|h_{2,1}\right|^2+\left|h_{2,2}\right|^2\right)\left(\left|h_{2,3}\right|^2+\left|h_{2,4}\right|^2\right)\right]}{3\left(\left|h_{1,1}\right|^2+\left|h_{1,2}\right|^2+\left|h_{1,3}\right|^2+\left|h_{1,4}\right|^2+\left|h_{2,1}\right|^2+\left|h_{2,2}\right|^2+\left|h_{2,3}\right|^2+\left|h_{2,4}\right|^2\right)^2}.$$

References

[1] LARSSON E G, EDFORS O, TUFVESSON F, et al. Massive MIMO for next generation wireless systems [J]. IEEE communications magazine, 2014, 52(2): 186 – 195. DOI: 10.1109/MCOM.2014.6736761
[2] HAN C, JORNET J M, AKYILDIZ I. Ultra-massive MIMO channel modeling for graphene-enabled terahertz-band communications [C]//2018 IEEE 87th Vehicular Technology Conference (VTC Spring). IEEE, 2018: 1 – 5
[3] HUANG C W, ZAPPONE A, ALEXANDROPOULOS G C, et al. Reconfigurable intelligent surfaces for energy efficiency in wireless communication [J]. IEEE transactions on wireless communications, 2019, 18(8): 4157 – 4170. DOI: 10.1109/TWC.2019.2922609
[4] WU Q, ZHANG R. Intelligent reflecting surface enhanced wireless network via joint active and passive beamforming [J]. IEEE transactions on wireless communications, 2019, 18(11): 5394 – 5409
[5] TANG W K, CHEN M Z, CHEN X Y, et al. Wireless communications with reconfigurable intelligent surface: Path loss modeling and experimental measurement [J]. IEEE transactions on wireless communications, 2021, 20(1): 421 – 439. DOI: 10.1109/TWC.2020.3024887
[6] TAO Q, WANG J W, ZHONG C J. Performance analysis of intelligent reflecting surface aided communication systems [J]. IEEE communications letters, 2020, 24(11): 2464 – 2468. DOI: 10.1109/LCOMM.2020.3011843
[7] CUI T J, QI M Q, WAN X, et al. Coding metamaterials, digital metamaterials and programmable metamaterials [J]. Light: science & applications, 2014, 3 (10): 218. DOI: 10.1038/lsa.2014.99
[8] CUI T J, LIU S, ZHANG L. Information metamaterials and metasurfaces [J]. Journal of materials chemistry, 2017, 5(15): 3644 – 3668. DOI: 10.1039/c7tc00548b
[9] ZHANG L, CHEN X Q, LIU S, et al. Space-time-coding digital metasurfaces [J]. Nature communications, 2018, 9(1): 1 – 11. DOI: 10.1038/s41467-018-06802-0
[10] ZHAO J, CHENG Q, CHEN J, et al. A tunable metamaterial absorber using varactor diodes [J]. New journal of physics, 2013, 15(4): 043049. DOI: 10.1088/1367-2630/15/4/043049
[11] HAN Y, TANG W K, JIN S, et al. Large intelligent surface-assisted wireless communication exploiting statistical CSI [J]. IEEE transactions on vehicular technology, 2019, 68(8): 8238 – 8242. DOI: 10.1109/TVT.2019.2923997
[12] DI RENZO M, ZAPPONE A, DEBBAH M, et al. Smart radio environments empowered by reconfigurable intelligent surfaces: How it works, state of research, and the road ahead [J]. IEEE journal on selected areas in communications, 2020, 38(11): 2450 – 2525. DOI: 10.1109/JSAC.2020.3007211
[13] ZHAO J, YANG X, DAI J Y, et al. Programmable time-domain digital-coding metasurface for non-linear harmonic manipulation and new wireless communication systems [J]. National science review, 2018, 6(2): 231 – 238. DOI: 10.1093/nsr/nwy135
[14] TANG W K, LI X, DAI J Y, et al. Wireless communications with programmable metasurface: transceiver design and experimental results [J]. China communications, 2019, 16(5): 46 – 61. DOI: 10.23919/j.cc.2019.05.004
[15] DAI J Y, TANG W K, ZHAO J, et al. Wireless communications through a simplified architecture based on time-domain digital coding metasurface [J]. Advanced materials technologies, 2019, 4(7): 1900044. DOI: 10.1002/admt.201900044
[16] TANG W K, DAI J Y, CHEN M Z, et al. Programmable metasurface-based RF chain-free 8PSK wireless transmitter [J]. Electronics letters, 2019, 55(7): 417 – 420. DOI: 10.1049/el.2019.0400
[17] TANG W K, DAI J Y, MING Z C, et al. Realization of reconfigurable intelligent surface-based alamouti space-time transmission [C]//Proceedings of 2020 International Conference on Wireless Communications and Signal Processing (WCSP). IEEE, 2020: 904 – 909. DOI: 10.1109/WCSP49889.2020.9299726
[18] KE J C, DAI J Y, CHEN M Z, et al. Linear and nonlinear polarization syntheses and their programmable controls based on anisotropic time-domain digital coding metasurface [J]. Small structures, 2021, 2(1): 2000060. DOI: 10.1002/sstr.202000060
[19] CHEN X Y, KE J C, TANG W K, et al. Design and implementation of MIMO transmission based on dual-polarized reconfigurable intelligent surface [J]. IEEE wireless communications letters, 2021, 10(10): 2155 – 2159. DOI: 10.1109/LWC.2021.3095172
[20] HAN Y, LI X, TANG W K, et al. Dual-polarized RIS-assisted mobile commu-

nications [J]. IEEE transactions on wireless communications, 2022, 21(1): 591 – 606. DOI: 10.1109/TWC.2021.3098521
[21] PATIL S T, SHINDE P N. A review of space-time block codes from real and complex orthogonal designs [J]. International journal of computer applications, 2014, 100(11): 16 – 19. DOI: 10.5120/17568-8239
[22] LI K, WANG Z. Analysis of space-time block coding (STBC) performance in MIMO system [J]. Wireless communication technology, 2008, 17(4): 11 – 16
[23] CHO K, YOON D. On the general BER expression of one- and two-dimensional amplitude modulations [J]. IEEE transactions on communications, 2002, 50(7): 1074 – 1080. DOI: 10.1109/TCOMM.2002.800818

Biographies

ZHOU Mingyong received his B. S. degree in communication engineering from the School of Communication and Information Engineering, Nanjing University of Posts and Telecommunications, China in 2020. He is currently pursuing his M.S. degree with the National Mobile Communications Research Laboratory, Southeast Unversity, China. His research interests include metasurface-based wireless communication system design and implementation.

CHEN Xiangyu received his B.S. degree in information engineering from the School of Information Science and Engineering, Southeast University, China in 2019. He is currently pursuing his M.S. degree with the National Mobile Communications Research Laboratory, Southeast Unversity. His research interests include metasurface-based wireless communication system design and measurement.

TANG Wankai received his B.S. degree in information engineering, M.S. degree in circuits and systems, and Ph.D. degree in communications and information systems from Southeast University, China in 2011, 2014, and 2021, respectively. He worked at National Instruments (Shanghai), USA from 2014 to 2016. He received the Electronics Letters Best Paper Award in 2020 and the China Communications Best Paper Award in 2021. His research interests include modeling and prototyping of metasurface-based wireless communication systems.

KE Jun Chen received his B.S. degree from the School of Instrument Science & Engineering, Southeast University, China in 2016, where he is currently pursuing his Ph.D. degree with the State Key Laboratory of Millimeter Waves, Department of Radio Engineering, Southeast University, China. His research interests include metamaterials, metasurfaces, and array antennas.

JIN Shi (jinshi@seu.edu.cn) received his Ph.D. degree in communications and information systems from Southeast University, China in 2007. From June 2007 to October 2009, he was a research fellow with the Adastral Park Research Campus, University College London, United Kingdom. He is currently with the faculty of the National Mobile Communications Research Laboratory, Southeast University. His research interests include space-time wireless communications, information theory, intelligent communications, and reconfigurable intelligent surfaces. He and his coauthors received the 2010 Young Author Best Paper Award from the IEEE Signal Processing Society and the 2011 IEEE Communications Society Stephen O. Rice Prize Paper Award in the field of communication theory.

CHENG Qiang received his B.S. and M.S. degrees from Nanjing University of Aeronautics and Astronautics, China in 2001 and 2004, respectively, and his Ph.D. degree from Southeast University, China in 2008. He is currently a full professor with the State Key Laboratory of Millimeter Waves, Southeast University. His research interests include metamaterials, tunable microwaves circuits, microwave imaging, and terahertz systems. He was a recipient of the 2010 Best Paper Award from *New Journal of Physics*. He was awarded China's Top Ten Scientific Advances of 2010 and the second class National Natural Science Award in 2014.

CUI Tie Jun received his B.S., M.S., and Ph.D. degrees in electrical engineering from Xidian University, China in 1987, 1990, and 1993, respectively. In 1993, he joined the Department of Electromagnetic Engineering, Xidian University, and was promoted to associate professor in 1993. From 1995 to 1997, he was a research fellow with the Institut fur Hochstfrequenztechnik und Elektronik, University of Karlsruhe, Germany. In 1997, he joined the Center for Computational Electromagnetics, Department of Electrical and Computer Engineering, University of Illinois at Urbana-Champaign, USA, first as a postdoctoral research associate and then as a research scientist. In 2001, he was a Cheung-Kong Professor with the Department of Radio Engineering, Southeast University, China. Currently he is the Chief Professor of Southeast University. He is also the founding director of the Institute of Electromagnetic Space, Southeast University. His current research interests include metamaterials and computational electromagnetics. He has published over 500 peer-review journal papers, which have been cited more than 40 000 times (H-Factor 102; Google Scholar). He is the Academician of the Chinese Academy of Science.